scientific reports

Check for updates

OPEN

CARG-2020 targets IL-12, IL-17, and PD-L1 pathways to effectively treat melanoma and breast cancer

Elham Ahmadi[1,2,4], Conner Chiari[1,4], Bhaskara Reddy Madina[2], Timur Olegovich Yarovinsky[2], Marie Marthe Krady[2], Ju Chen[1,3], Bijan Almassian[2], Valerian Nakaar[2] & Kepeng Wang[1]✉

Cancer immunotherapy has recently achieved a breakthrough status, however, it is not effective in all cancer types. Genetically engineered oncolytic viruses (OVs) with immunomodulators are promising new therapeutic modalities for cancer. CARG-2020 is an engineered trivalent oncolytic viral construct that specifically expresses three immune modulators that inhibit IL-17RA signaling and regulate PD-L1 expression by shRNAs, along with the cytokine IL-12 which activates multiple tumoricidal pathways. Previous work showed that intratumoral (*i.t.*) injection of CARG-2020 exhibits robust efficacy against established colorectal cancer (CRC). In this study, we report that systemic delivery of CARG-2020 via the intravenous (*i.v.*) route can successfully control CRC growth. To further expand the scope of CARG-2020 as a pan-cancer candidate, we also show that CARG-2020 works in two additional mouse models of melanoma and triple-negative breast cancer. Administration of CARG-2020 resulted in increased accumulation of CD8⁺ T lymphocytes in the tumors, and depletion of these T cells results in poor tumor regression mediated by CARG-2020. Overall, our study shows a broad-spectrum efficacy of CARG-2020 in solid tumors and demonstrates the potential of CARG-2020 to be developed as a clinical candidate for the treatment of multiple human cancers that are surgically accessible.

Keywords Oncolytic virus, Cancer immunotherapy, Interleukin-12, Interleukin-17, PD-L1

Viral vectors have been explored for the treatment of cancers in the past decades and have had limited success[1]. There are only two FDA-approved oncolytic viral therapies in the US. First, T-VEC, derived from type 1 herpes simplex virus carrying the granulocyte macrophage colony-stimulating factor (GM-CSF), is used for the treatment of metastatic melanoma[2]. Second, a more recent success highlights the use of non-replicative adenovirus to deliver human interferon a-2b through an intravesical route for the treatment of BCG-unresponsive non-muscle-invasive bladder cancer[3]. Multiple novel oncolytic viral agents are under development, with many carrying immune-modulating payloads, such as GM-CSF, to enhance anti-tumor immunity[1,4]. In addition, oncolytic viral therapies may be administered alone or in combination with other therapies for cancers, notably immune checkpoint inhibitors[4]. As more pathways involved in the activation and persistence of anti-cancer immunity are discovered, there is a general trend to target multiple pathways simultaneously to enhance the efficacy of cancer immunotherapies. Another avenue to increase the efficacy of oncolytic viral agents is systemic delivery which is also an area under active investigation[1,4].

In our recent studies, we combined the oncolytic virus-like vesicle (VLV) platform with immunomodulatory payloads targeting IL-12, IL-17, and PD-L1 pathways simultaneously. VLV is a self-amplifying RNA replicon vector designed by combining Semliki Forest virus (SFV) RNA-dependent polymerase and vesicular stomatitis virus glycoprotein (VSV-G)[5–7]. Additionally, VLVs can co-express different payloads from multiple subgenomic regions[8–11]. Among the payloads of CARG-2020, IL-12 is a heterodimeric protein containing p35 and p40 subunits that potently stimulates Th1 immunity[12,13]. Following IL-12 stimulation, antigen-engaged CD4⁺ T cells differentiate into IFN-γ producing T helper type 1 cells[12]. These T cells in turn aid anti-cancer immunity by activating tumor infiltrating CD8⁺ T cells, NK cells, dendritic cells, among others[14]. This cytokine has been explored for the treatment of cancers, but its clinical use through systemic injection has been halted owing to severe toxicity in patients[15–20]. Therefore, the use of IL-12 for cancer immunotherapy has largely focused on the local delivery of cytokines[20]. Similarly, IL-17 family of cytokines plays important roles in resistance to pathogen infection[21]; however, Interleukin-17 (IL-17) family of cytokines can also promote tumor development in multiple

[1]Department of Immunology, School of Medicine, University of Connecticut Health Center, Farmington, CT 06030, USA. [2]CaroGen Corporation, Farmington, CT 06030, USA. [3]The Eighth Clinical Medical College of Guangzhou University of Chinese Medicine, Foshan Hospital of Traditional Chinese Medicine, Foshan 528000, Guangdong, China. [4]Elham Ahmadi and Conner Chiari have contributed equally to this work. ✉email: kewang@uchc.edu

organs[22]. For instance, IL-17 A, C and F promote the development of CRCs[23–27]. Ablation of IL-17 signaling also slows the metastatic growth of breast cancer[28]. Furthermore, we recently found a role for IL-17 in inhibiting the infiltration of $CD8^+$ T cells into tumors by downregulating CXCL9 family chemokines[29], suggesting a potentially synergistic effect of blocking IL-17 on top of other cancer immunotherapies, such as anti-PD-1 or PD-L1 agents that rescue tumor-infiltrating T cells from exhaustion[30]. Therefore, we incorporated an extracellular domain of IL-17RA into CARG-2020 to serve as an antagonist of IL-17 signaling[31]. Further incorporation of PD-L1 shRNAs reduces the expression of PD-L1[31]. PD-L1 signals via its cognate receptor PD-1 on tumor-infiltrating T cells to inhibit effector T cell function, while enhancing the activity of regulatory T cells[32]. The blockade of this pathway has thus far shown great promise in the treatment of multiple cancers[30,33]. Based on this evidence, we chose to incorporate IL-12, IL-17RA antagonist, and PD-L1 shRNAs into CARG-2020, with the expectation of generating a synergistic outcome whereby IL-12 initiates Th1 armed immunity for cancer therapy; blockade of IL-17 sustains such immunity by preventing cancer promoting inflammation and permitting $CD8^+$ T cell influx; and blockade of PD-L1 prevents its inhibition on effector T cells with a resultant T cell exhaustion.

With the three immune-modulating payloads, CARG-2020 effectively remodels or "heats up" the tumor microenvironment (TME), induces complete tumor regression, generates immune memory, and protects against future tumor recurrence as observed in our previous studies using mouse models of colon and ovarian cancers[31,34]. Treatment of established colorectal tumors in mice with CARG-2020 resulted in marked inhibition of tumor growth, eradication of most tumors, and long-lasting immune memory in the host[31]. Intratumoral injection of CARG-2020 also mounted abscopal effects against distal and untreated tumors while eliciting strong Th1-armed immunity[31]. Gene profiling data suggest that CARG-2020 modulates the IL-12, IL-17, and PD-L1 signaling pathways and regulates tumor-promoting inflammation, immune suppression, T cell exhaustion, cancer stemness, and oncogenic signaling[31]. In an independent study, intraperitoneal injection of CARG-2020 induced transferable immune memory to regulate recurrent Ovarian carcinomatosis[34]. While these studies provide important insights into the efficacy of CARG-2020 in colorectal and ovarian cancers, it is not clear if the novel agent can be applied to other cancer types or administered through different routes.

In this study, we employed mouse models of CRC, triple-negative breast cancer (TNBC), as well as a model of melanoma. CARG-2020 treatments via intravenous and intratumoral routes showed robust efficacy. We also established that $CD8^+$ T cells play a vital role in the efficacy of CARG-2020. In addition, the direct treatment of multiple solid tumors with CARG-2020 elicited robust anti-tumor therapeutic efficacy, which demonstrates the potential of CARG-2020 for widespread clinical applications in the future.

Materials and methods

Generation of VLV-based constructs

CARG-2020 and control constructs have been described previously[31]. Briefly, a single chain of IL-12 was generated by linking IL-12p40 and IL-12p35 with an elastic linker. cDNA encoding the single-chain IL-12 was cloned into the VLV dp-VSV G^{NJ} vector. CARG-2020 incorporated an extracellular portion of IL-17RA, serving as an antagonist of IL-17 signaling, and three shRNAs against PD-L1 to knock down PD-L1 expression. As a control, GFP was cloned into the VLV dp-VSV G^{NJ} vector instead of the three payloads.

VLV production

To produce VLV stocks, BHK-21 cells (ATCC CCL 10) were cultured in Dulbecco's modified Eagle's medium (DMEM) supplemented with 5% fetal bovine serum (FBS). VLVs were produced by transfecting BHK-21 cells with VLV plasmid DNA, followed by collection of the master VLV stock. Propagation of the working stocks was performed by single passage of the master stock in BHK-21 cells cultured in Opti-MEM™ Reduced Serum Medium (Thermo Fisher, Waltham, MA, USA). Working stocks were concentrated using MacroSep® Advance 100 K centrifugal devices (Pall Laboratories, Port Washington, NY, USA) in a swinging bucket centrifuge. VLV titers were determined using serial dilutions and a standard 2-d plaque assay on BHK-21 cell monolayers as previously described[7]. The VLVs plaques were counted using a dissecting microscope.

Animal models

C57BL/6J mice were obtained from the Jackson Laboratory. All mice were maintained in specific-pathogen-free conditions in filter-topped cages on autoclaved food and water at UConn Health. All experiments used co-housed, gender-matched littermates to ensure the consistency of common microflora. Both male and female mice were used for all experiments, except for mouse model of breast cancer, where only female mice were used. At the end of the experiments, mice were euthanized by CO_2 anesthesia followed with cervical dislocation. All animal experiments were approved by the IACUC of UConn Health, and performed in accordance with the relevant guidelines and regulations including the ARRIVE guidelines.

Tumor immunotherapy models

MC38 colon cancer cell line was purchased from MilliporeSigma (Cat # SCC172). B16 melanoma cells were from ATCC (Cat # CRL-6475). PY8119 breast cancer cell line was from Dr. Weizhou Zhang at the University of Florida. These cells were cultured in DMEM supplemented with 10% FBS, penicillin, and streptomycin. For mouse models of colon cancer and melanoma, 500,000 cultured MC38 and B16 cells were digested with trypsin, suspended in PBS, and injected subcutaneously into the flanks of 2–3 months old C57BL/6J mice. Equal numbers of male and female mice were used in the tests, and the mice were randomly assigned to different treatment groups. For mouse models of breast cancers, 500,000 PY8119 cells were grafted into the second mammary fat pad of adult female C57BL/6J mice. Tumor length and width were measured every three days using a caliper. Tumor volume was calculated as $V = (\text{Length} \times \text{Width}^2)/2$. VLVs were administered intratumorally or intravenously at a dose of 5×10^7 PFU per injection at the indicated time points. Depleting antibodies against CD4 (Bio X Cell #

BE0003), CD8α (Bio X Cell # BE0061) and NK1.1 (Bio X Cell # BE0036) were given intraperitoneally at a dose of 200 μg per injection at indicated time points. The control antibody (Bio X Cell # BE0083) was administered to the other groups. Mice were sacrificed at the indicated time points for analyses or continuously followed for tumor growth until their tumor volume reached 3 cm^3, at which point they were sacrificed.

To test immune memory following CARG-2020 treatment, mice that showed B16 melanoma tumor eradication were re-challenged with the same tumor grafting scheme 101 days following the last dose of CARG-2020 injection, and were followed up for tumor growth. As a control, naïve C57BL/6 mice were also grafted with B16 melanoma tumor cells at the same time.

Flow cytometry

Mouse MC38 colorectal tumors and B16 melaonomas were minced with scissors and digested with 1 mg/kg collagenase IV (Sigma Aldrich, Cat # C5138) for 20 min. Cells were filtered through a 70-μm cell sieve and stained with Live/Dead fixable exclusion dye (Tonbo Bioscience, Cat # 13–0868), followed by fluorochrome-conjugated antibodies in PBS with 2% fetal bovine serum (FBS) and 1mM EDTA. Anti-CD3 (Cat # 100206), anti-CD4 (Cat # 100536), anti-CD45 (Cat # 103138), anti-NK1.1 (Cat # 156503), anti-IFN-γ (Cat # 505808) and anti-CD335 (Cat # 137605) antibodies were purchased from BioLegend. Anti-CD8α (Cat # 558106), anti-CD3e (Cat # 612771), anti-CD4 (Cat # 557956), anti-CD8a (Cat # 558106), anti-Ly6C (Cat # 570134), anti-Ly6G (Cat # 565964) were purchased from BD Biosciences. Anti-CD62L (Cat # 47-0621-82) and anti-CD44 (Cat # 12-0441-82) were purchased from Invitrogen. For intracellular cytokine staining, cells were stimulated with Cell Stimulation Cocktail (eBioscience, Cat # 00-4975-93) for 4 h, followed with fixation and staining with Foxp3/transcription factor staining buffer set (eBioscience, Cat # 00-5523-00).

Flow cytometry was performed using a BD LSRII and BD FACSYMPHONY A5 SE flow cytometers. Data were analyzed using FlowJo software.

qRT-PCR

Tissues from primary tumors and different organs were harvested for RNA extraction (Qiagen, Cat # 74106). cDNA was synthesized using the Bio-Rad iScript Advanced cDNA Synthesis Kit (Bio-Rad, Cat # 1708891). qPCR was performed to quantify the mRNAs levels of the indicated genes on a BioRad CFX96 real-time PCR machine using SsoAdvanced Universal SYBR Green Supermix (Bio-Rad Cat # 1725275). RPL32 RNA was used as an internal control. The data were calculated as $2^{(Ct(RPL32-\text{gene of interest}))}$ to compare experimental groups to controls and are presented in arbitrary units. The primer sequences are listed in Table 1. Whenever possible, primers were intron-spanning, such that amplification was only feasible on complementary DNA but not on genomic DNA.

Statistical analysis

Statistical analysis was performed using GraphPad Prism version 9 (GraphPad Software, San Diego, CA, USA), unless stated otherwise. Data were analyzed by the unpaired Students' t-test for pair-wise comparisons without assuming equal variance, and one-way ANOVA for comparison between three or more groups. A p value below 0.05 was considered significant. Tumor growth trends among the different treatment groups were compared and analyzed using a two-way ANOVA. Survival data were analyzed using the log-rank test. Unless otherwise stated, n is the number of biological replicates (individual mice and organs).

Results

CARG-2020 is effective when given systemically

CARG-2020 is based on the virus-like vesicle backbone and incorporates a single chain IL-12, a dominant negative form of IL-17RA, and three shRNAs against PD-L1 as immune-modulating payloads (Fig. 1a)[31,34]. As controls, this study also employed VLV that carry individual payloads including GFP, IL-12, IL-17RA antagonist, and PD-L1 shRNAs (Fig. 1a). We have previously shown that intratumoral injection of CARG-2020 effectively eradicates the majority of grafted MC38 tumors[31]. In clinical practice, this will require direct injection of CARG-2020 into surgically accessible tumors. To fill a major clinical gap, we tested the possibility of administering CARG-2020 via systemic circulation. For this purpose, we examined the biodistribution of VLV vectors by grafting mice with MC38 tumors, and injecting VLV-GFP through intratumoral and intravenous routes (Fig. 1b). The distribution of VLV was quantified by RT-qPCR using GFP RNA as a marker. Direct tumor injection of VLV achieved high local exposure, whereas VLVs injected *i.v.* were predominantly located in the

Primer	Reverse	Forward
RPL32	TTGTGAGCAATCTCAGCACA	GGGAGCAACAAGAAAACCAA
GFP	TGCTCAGGTAGTGGTTGTCG	AGAACGGCATCAAGGTGAAC
IFN-γ	TGAACGCTACACACTGCATCT	GACTCCTTTTCCGCTTCCTGA
Granzyme B	CTCTCGAATAAGGAAGCCCC	CTGACCTTGTCTCTGGCCTC
TNF-α	GGTGATCGGTCCCCAAAGG	CCAGCTGCTCCTCCACTTG
PD-1	CTGCAGTTGAGCTGGCAATC	CCTCTGACACTGTGAGCCAG
Perforin	TAGCCAATTTTGCAGCTGAG	TGGAGGTTTTTGTACCAGGC

Table 1. Primer Sequences for Q-PCR.

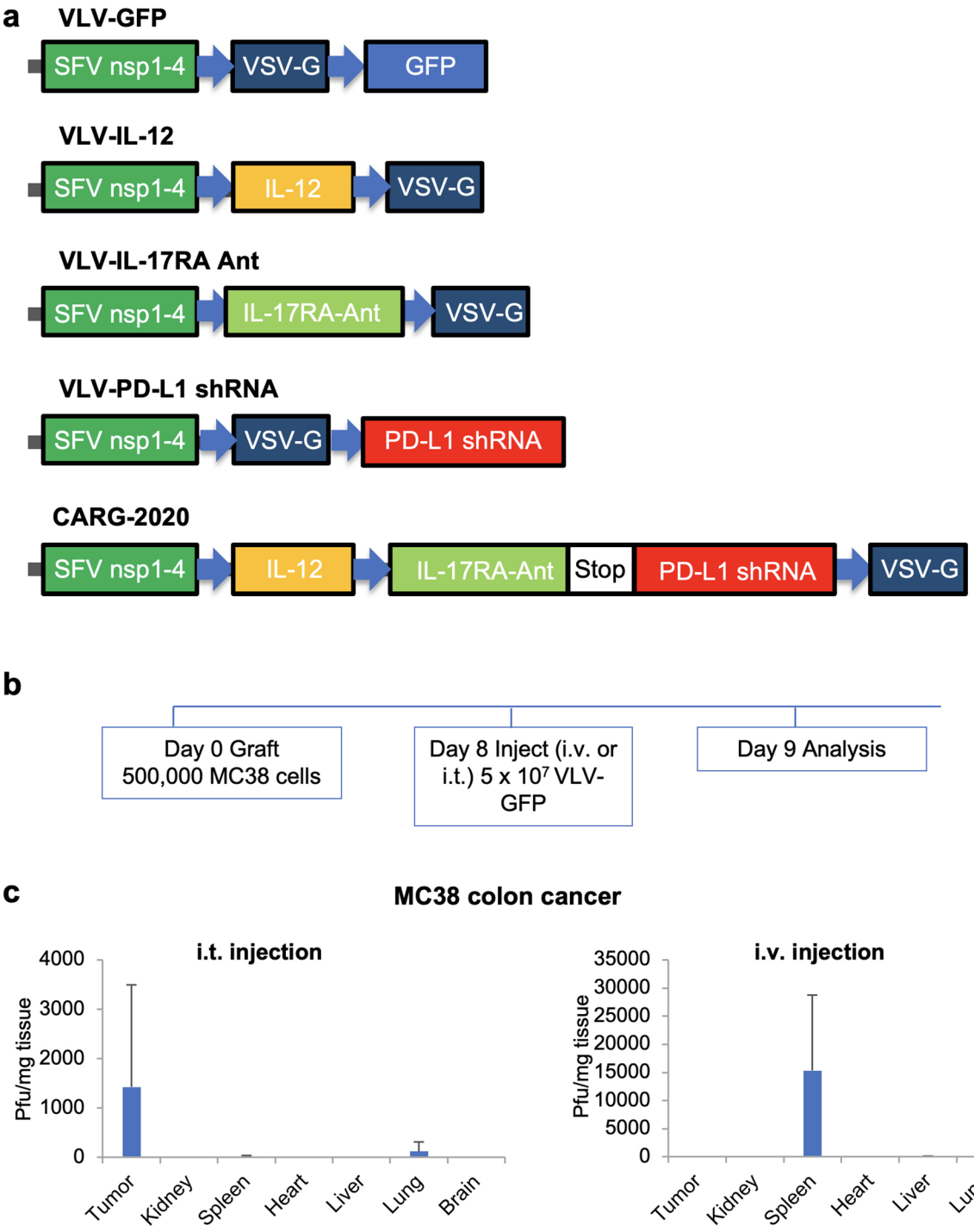

Fig. 1. Design of CARG-2020 and biodistribution of systemically delivered VLV. **a** CARG-2020 was designed based on the virus-like vesicle (VLV) platform, which includes non-structural proteins from Semliki Forest virus, and glycoprotein of vesicular stomatitis virus. CARG-2020 incorporates a single chain, biologically active IL-12, an extracellular domain of IL-17RA serving as an antagonist, and three shRNAs against PD-L1. As controls, we also designed VLV that carry single payloads such as GFP (VLV-GFP), IL-12 (VLV-IL-12), IL-17RA antagonist (VLV-IL-17RA Ant), and shRNAs against PD-L1 (VLV-PD-L1 shRNA). **b-c**, 500,000 MC38 tumors were grafted into the flank of C57BL/6J mice. 5×10^7 pfu VLV-GFP was injected directly into the tumor (*i.t.* injection, left panel) or through the retro-orbital route (*i.v.* injection, right panel). One day later, mice were sacrificed, and their tumors and different organs were harvested for RT-qPCR analysis on the level of GFP RNA. A serial dilution of VLV-GFP was used to build a standard curve. Data were depicted as the average equivalent pfu of VLV-GFP in mg tumor/normal tissues +/- S.D, $n = 7$.

spleen and lungs, with a low level of GFP mRNA detected in MC38 tumors (Fig. 1c). Less than 2% of all VLVs injected via *i.v.* route homed to the tumor (Fig. 1c). Next, we sought to test whether systemic delivery of the GFP-control or multivalent agent resulted in effective tumor control. To this end, we grafted MC38 tumors into mice, and injected CARG-2020 intravenously (Fig. 2a). Delivery of CARG-2020 via *i.v.* route resulted in marked inhibition of the growth of established MC38 tumors (Fig. 2b, c). Upon long-term follow-up, three out of the 11 mice treated with *i.v.* injection of CARG-2020 became tumor-free, whereas none of the mice in the control group (treated with VLV-GFP) survived (Fig. 2d). Under this treatment scheme, we did not observe significant changes in body weight or treatment-related deaths in the animals, indicating a tolerable profile of CARG-2020 when delivered *i.v.* (Fig. 2e).

We next set out to test the safety boundary of *i.v.* injected CARG-2020 for cancer treatment. To this end, we compared CARG-2020 with VLV-GFP and VLV-IL-12, the latter carries only IL-12 as a payload. Under the same treatment scheme, both CARG-2020 and VLV-IL-12 showed good control of tumor growth following the initial injections (Fig. 3a). However, *i.v.* injections of VLV-IL-12 resulted in treatment-related deaths in mice following the third dose, whereas the same dose of CARG-2020 resulted in the deaths of several animals following dose #5 (Fig. 3b). These results indicate that CARG-2020 has a better safety profile compared to VLV-IL-12 when injected *i.v.*, possibly due to the larger payload which results in slower replication of the construct (data not shown). Nonetheless, the loss of experimental animals following repeated doses of CARG-2020 demonstrates its unspecific distribution during systemic injection (Fig. 1c), and therefore requires caution to be exercised during systemic delivery.

The efficacy of systemically delivered CARG-2020 likely stemmed from the activation of T lymphocytes, which migrate into the tumors to initiate anti-tumor function. In order to test this hypothesis, we injected VLV-GFP and CARG-2020 via *i.v.* administration to MC38 tumor bearing mice to interrogate the status of T cell activation in the tumors (Fig. 4a). Supporting our hypothesis, it was found that systemic delivery of CARG-2020 resulted in an upregulation in the number of activated $CD8^+$ cytotoxic T lymphocytes in the tumor (Fig. 4b, c). Overall, these data indicate that systemic *i.v.* injection of CARG-2020 is effective against established colon tumors through the activation of $CD8^+$ T cells.

CARG-2020's efficacy against colorectal cancer is dependent on $CD4^+$ and $CD8^+$ T cells

Our previous studies have shown the marked efficacy of CARG-2020 against established tumors in various models, including the MC38 colon, BNLT3 liver, and triple knockout ovarian tumors[31,34]. Intratumoral injection of CARG-2020 in the MC38 model also significantly increased the number of IFN-γ-producing $CD4^+$ and $CD8^+$ cells in both tumors and spleens[31]. To test whether these cells are required for the efficacy of CARG-2020, we performed a similar *i.t.* injection of CARG-2020 into MC38 tumors and then depleted $CD4^+$ and $CD8^+$ T cells with neutralizing antibodies. Consistent with this notion, treatment with CARG-2020 suppressed colon tumor growth and resulted in tumor shrinkage (Fig. 5a, b). The depletion of $CD8^+$ T cells, and to a lesser extent, $CD4^+$ T cells, in mice treated with CARG-2020 reduced the efficacy of CARG-2020, suggesting that $CD8^+$, and to a lesser extent $CD4^+$, T cells play a key role in the action of CARG-2020 (Fig. 5a, b). In contrast, depletion of NK cells by an antibody against NK1.1, did not change the magnitude of tumor inhibition by CARG-2020 (Fig. 5a, b). We confirmed the successful depletion of these immune cell populations by flow cytometry analysis of splenocytes from control and antibody-treated animals (Fig. 5c).

CARG-2020 is effective against melanoma in mice

Next, we sought to expand the landscape in which the CARG-2020 may be used. One target is melanoma, which is surgically accessible for *i.t.* injections and has already been successfully treated with T-VEC[2]. To test the efficacy of CARG-2020 in melanoma, we grafted B16 melanoma cells subcutaneously into C57BL/6J mice and determined the optimal treatment dose by performing a dose-escalation study (Fig. 6a). A single *i.t.* injection of CARG-2020 showed dose-dependent inhibition of B16 tumor growth, but failed to cause tumor regression (Fig. 6b). To further test the potential of CARG-2020 in melanoma treatment, we injected six doses of CARG-2020 (Fig. 6c). We also compared CARG-2020 with direct injections of the four other VLV constructs (Fig. 1a). Only CARG-2020 treated mice showed tumor eradication (2 out of 6) (Fig. 6d). Compared to VLV-GFP and single payload VLVs, CARG-2020 treated mice also showed significantly prolonged survival, demonstrating the benefit of targeting all three pathways (IL-12, IL-17, and PD-L1) by the single agent (Fig. 6d). We further tested if CARG-2020 elicits effective anti-tumor memory in mice that had their tumor cured. To this end, we re-challenged the two mice that showed tumor eradication after CARG-2020 treatment with the same B16 melanoma grafting scheme 101 days after the last dose of CARG-2020. Neither of these mice showed signs of tumor regrowth, whereas all 5 control animals grew tumors following B16 graft (Fig. 6e).

To interrogate the mechanism by which CARG-2020 mounts an effective treatment against melanoma, we performed q-PCR and analyzed the expression levels of Th1-marker genes. Compared to melanoma tumors treated with VLV-GFP, CARG-2020 treated tumors showed upregulated expression of IFN-γ, perforin, TNF-α, Granzyme B, and PD-1, which are all markers of Th1 activation (Fig. 7a, b). Consistent with this notion, flow cytometry analysis on tumor-infiltrating immune cells showed increased proportion of $CD8^+$ T cells in the tumor following CARG-2020 treatment (Fig. 7c). This is likely caused by the delivery of IL-12 by CARG-2020, as VLV-IL-12 treated tumors showed a similar pattern of $CD8^+$ T cell increase (Fig. 7c).

CARG-2020 inhibits the growth of TNBC

We next sought to explore the use of CARG-2020 in breast cancer, which is one of the major cancer types in humans, with intratumoral injection being feasible. Among the subtypes of breast cancer, triple-negative breast cancer (TNBC) is characterized by rapid growth, aggressive clinical scores, early metastasis, and poor prognosis[35–37]. Currently, immunotherapy approaches, such as immune checkpoint blockade (ICB) treatment,

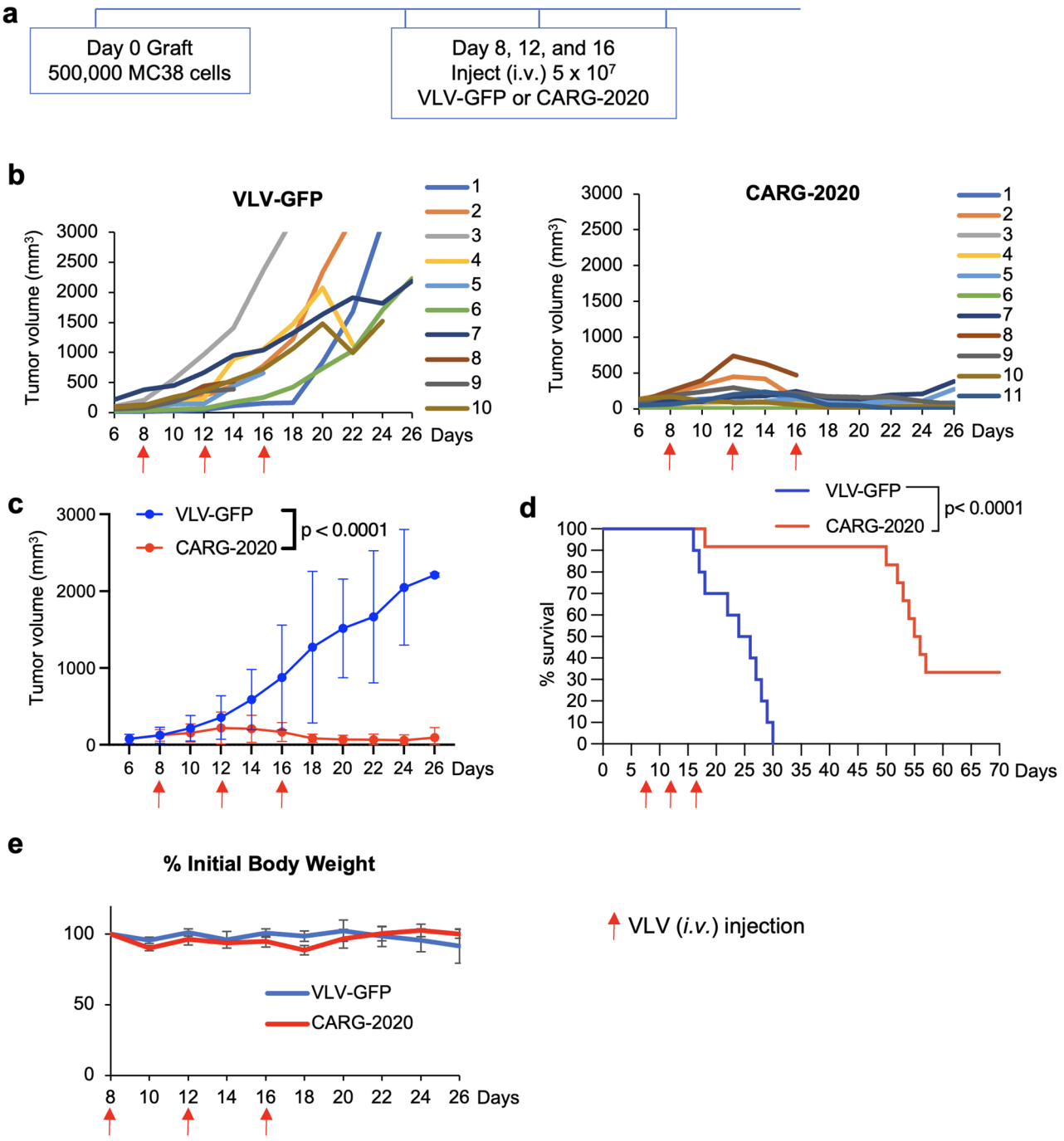

Fig. 2. CARG-2020 is effective against colon tumors when delivered i.v. **a**, MC38 colon tumor cells were grafted subcutaneously to the flank of C57BL/6J mice. Starting at day 8 since tumor graft, 5×10^7 pfu VLV-GFP and CARG-2020 were injected intravenously (*i.v.*) through the retro-orbital route every 4 days for a total of 3 doses. **b**, tumor sizes were measured and calculated every 2 days. Each line represents one individual animal. $N = 10$ for VLV-GFP and 11 for CARG-2020. **c**, average tumor volume of animals from each group with indicated treatments. Data were shown as average ± S.D. **d**, survival of mice under VLV-GFP or CARG-2020 treatment as percentages of initial numbers of mice. Mice with tumor sizes exceeding 3000 mm^3 were euthanized and counted toward deaths. **e**, average body weight of mice as percentages of initial body weight on day 8 when VLV treatment begins. Arrows indicate days of treatment.

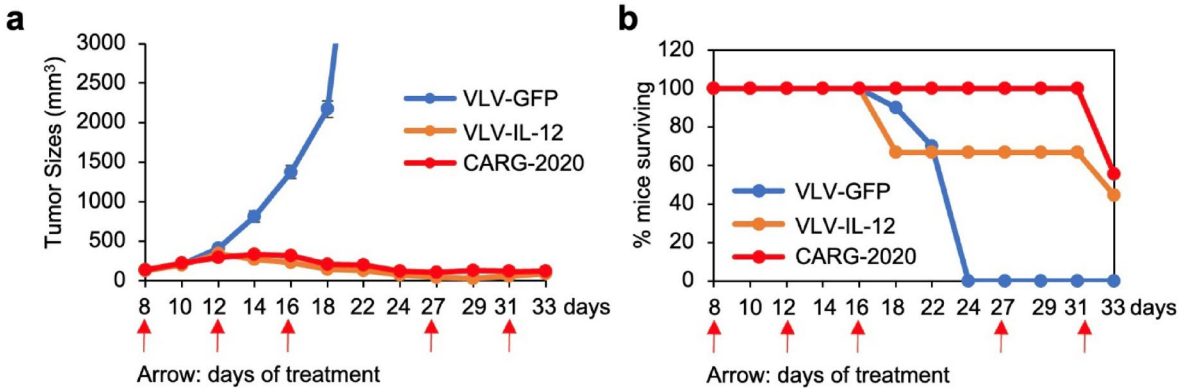

Fig. 3. CARG-2020 showed enhanced, but limited tolerance when delivered i.v. MC38 colon tumor cells were grafted subcutaneously to the flank of C57BL/6J mice. Starting at day 8 since tumor graft, 5×10^7 pfu VLV-GFP ($n = 10$), VLV-IL-12 ($n = 9$), and CARG-2020 ($n = 9$) were injected intravenously (*i.v.*) through the retro-orbital at indicated dates. **a** Average tumor volume of each treatment groups. **b** Percentages of mice surviving following different treatment schemes. Mice were euthanized when their tumors reached 3000 mm^3 in size, or showed signs of distress.

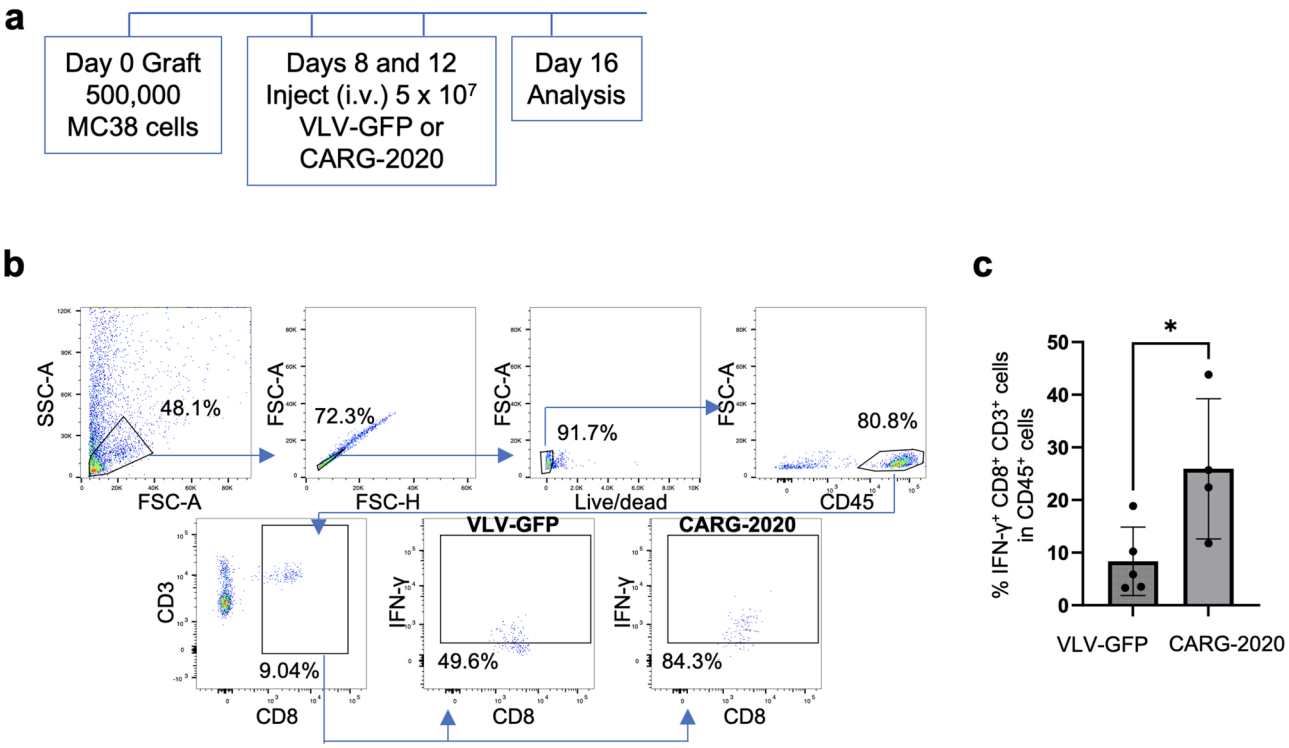

Fig. 4. CARG-2020 activates tumor-infiltrating $CD8^+$ T cells when delivered i.v. **a** MC38 colon tumor cells were grafted subcutaneously to the flank of C57BL/6J mice. Mice subsequently received two doses of VLV-GFP or CARG-2020 (5×10^7 pfu per dose, 4 days apart) via *i.v.* injection, and their tumors were dissociated into single cells and analyzed by flow cytometry 4 days after the second dose. **b** Representative flow cytometry gating scheme. **c** Quantification of the percentages of IFN-γ^+ $CD8^+$ T cells in all hematopoietic cells ($CD45^+$) in MC38 tumors. $N = 5$ for VLV-GFP, and $N = 4$ for CARG-2020. Data were shown as average +/- S.D. * $p < 0.05$.

Figure 5

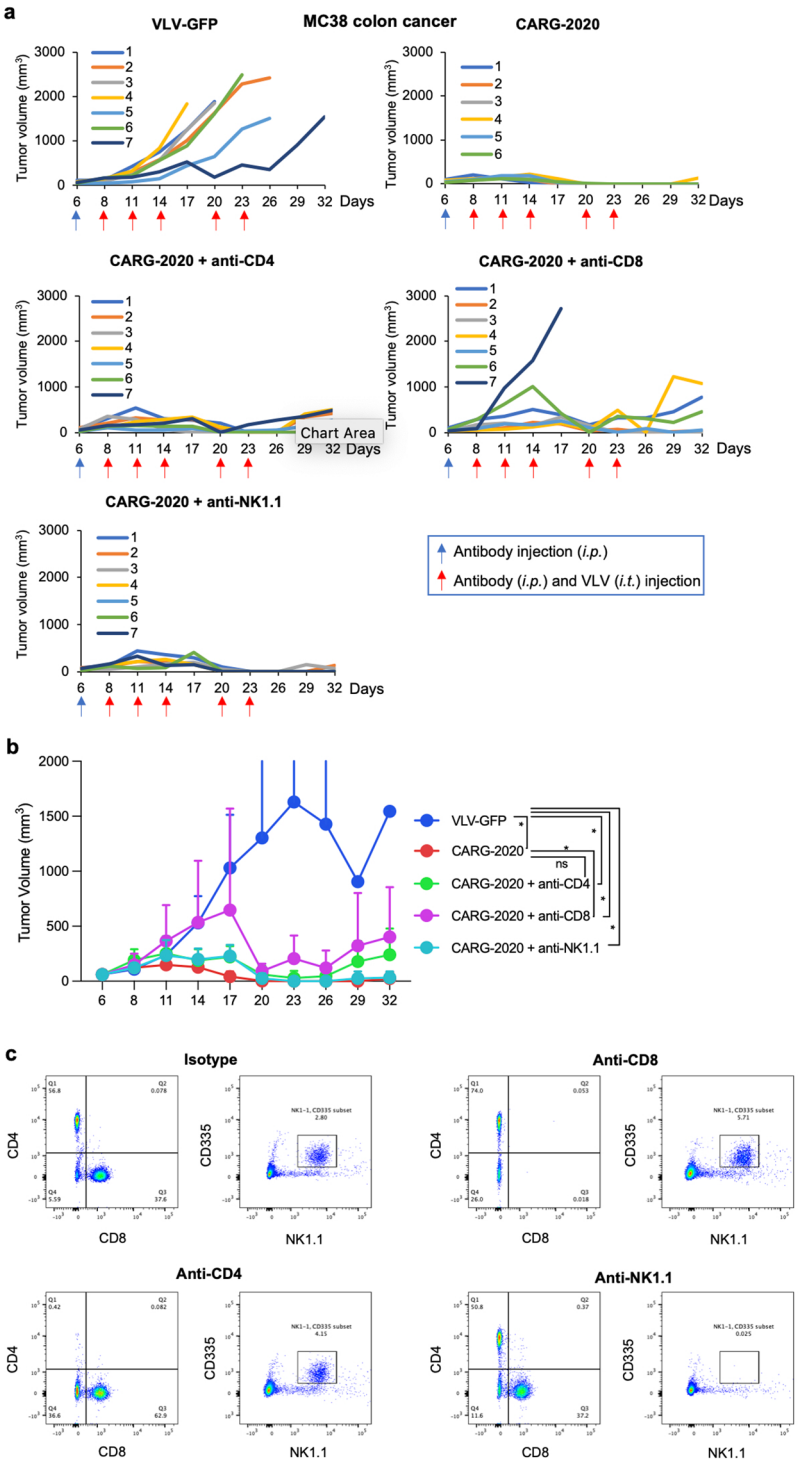

improve clinical outcomes; however, ICB therapies have serious side effects due to non-specific effects and on-target, off-tumor toxicity[38,39]. We employed the PY8119 mouse TNBC cell line and grafted these cells into the mammary fat pads of C57BL/6J mice. We tested the efficacy of CARG-2020 in this model and compared it with the blockade of PD-1 using a blocking antibody. While PD-1 blockade did not result in observable changes in the tumor growth rate, CARG-2020 treatment showed promising efficacy (Fig. 8a). This was also reflected in the prolonged survival of the mice receiving CARG-2020 (Fig. 8b). Immune checkpoint blockade treatment is less efficient in immunologically 'cold' tumors[40,41]. However, CARG-2020 engineered oncolytic virus selectively replicates within tumor cells and lyses them and in the process immunologically "heats up" the tumors. At the same time the vector delivers three immunostimulatory molecules to improve tumor regression efficacy[31,34]. Similar to what we observed previously, repeated *i.t.* injection of CARG-2020 into TNBC tumors did not result in loss of body weight in mice (Fig. 8c). Treatment with CARG-2020 also resulted in the increase in the expression

Fig. 5. CD4$^+$ and CD8$^+$ T cells mediate the therapeutic efficacy of CARG-2020. 500,000 MC38 colon tumor cells were grafted subcutaneously to the flank of C57BL/6J mice, and tumor sizes were measured every 2–3 days using a caliper. At day 6 after tumor graft, neutralizing antibodies against CD4, CD8α, or NK1.1 were given intraperitoneally (*i.p.*) at a dose of 200 μg per mouse. Isotype antibody was injected as a control. Starting at day 8, mice were treated with both intratumoral (*i.t.*) injection of VLV-GFP or CARG-2020 (5×10^7 pfu/injection) and intraperitoneal injection of antibodies. The blue arrow indicates treatment with antibody only (day 6), and red arrows indicates treatment with both antibodies and VLV agents. **a** Growth curve of tumors on each individual mouse in indicated treatment groups. **b** Average tumor volume of animals from each group with indicated treatments. * $p < 0.05$. **c**, C57BL/6J mice were treated with isotype, anti-CD4, anti-CD8α, or anti-NK1.1 antibodies, and their spleens were harvested 3 days after antibody injection and analyzed by flow cytometry. Cells were stained and gated on live/CD45$^+$/CD3$^+$ populations for CD8$^+$ and CD4$^+$ T cells, and live/CD45$^+$/CD3$^-$ populations for NK cells, which are also NK1.1$^+$ and CD335$^+$. Data represent consistent findings in 2 animals per group.

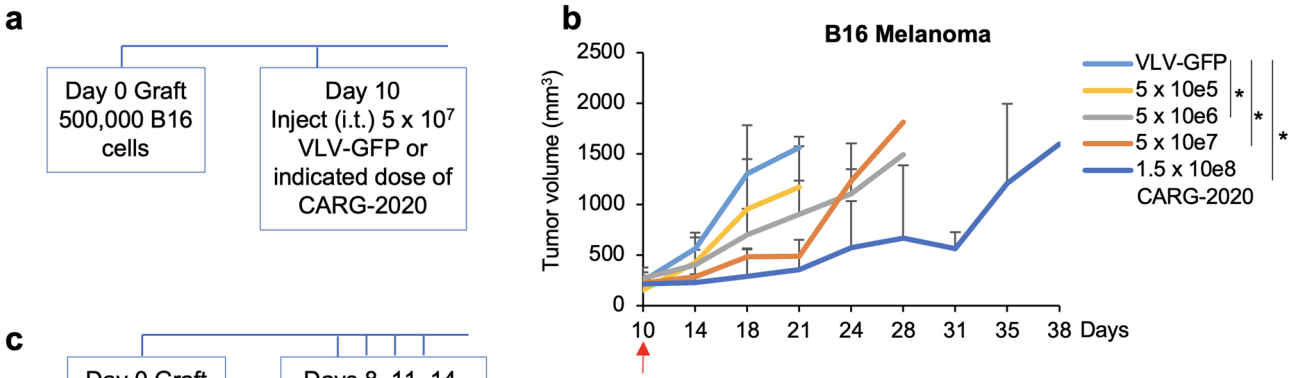

Hosts	Tumor growth following re-challenge
CARG-2020 cured	0/2
Naïve	5/5

Fig. 6. CARG-2020 is effective against melanoma in mice. **a**, **b** 500,000 B16 melanoma cells were grafted subcutaneously into the flank of C57BL/6J mice. 10 days after tumor graft, tumors received a single injection of indicated doses of CARG-2020. 5×10^7 pfu VLV-GFP was also injected to the control group. Tumor sizes were monitored at indicated dates and shown as average + S.D., $n = 7$. **c**, **d**, VLV-GFP, VLV-IL-12, VLV-IL-17RA Ant, VLV-PD-L1 shRNA, and CARG-2020 were injected intratumorally to B16 melanoma tumors at indicated dates and their tumors were examined and measured every three days. Mice were euthanized when their tumors reach 2000 mm^3, and the percentages of mice surviving are shown in **d**. **e** 101 days since the last dose of CARG-2020 injection, tumor-free mice resulting from the treatment were re-challenged with B16 melanoma grafting the same way as (**a**), and followed up for one month for tumor re-growth. As controls, naïve C57BL/6J mice were also grafted with B16 melanoma cells at the same time point. Fractions of mice that show tumor growth are shown. * $p < 0.05$.

of IFN-γ, perforin, TNF, Granzyme B, and PD-1 in the whole tumor, which are known to be upregulated in activated Th1 cells, CD8$^+$ T cells, and other immune cells (Fig. 8d). Taken together, our data demonstrate the robust therapeutic efficacy of CARG-2020 against TNBC in mice.

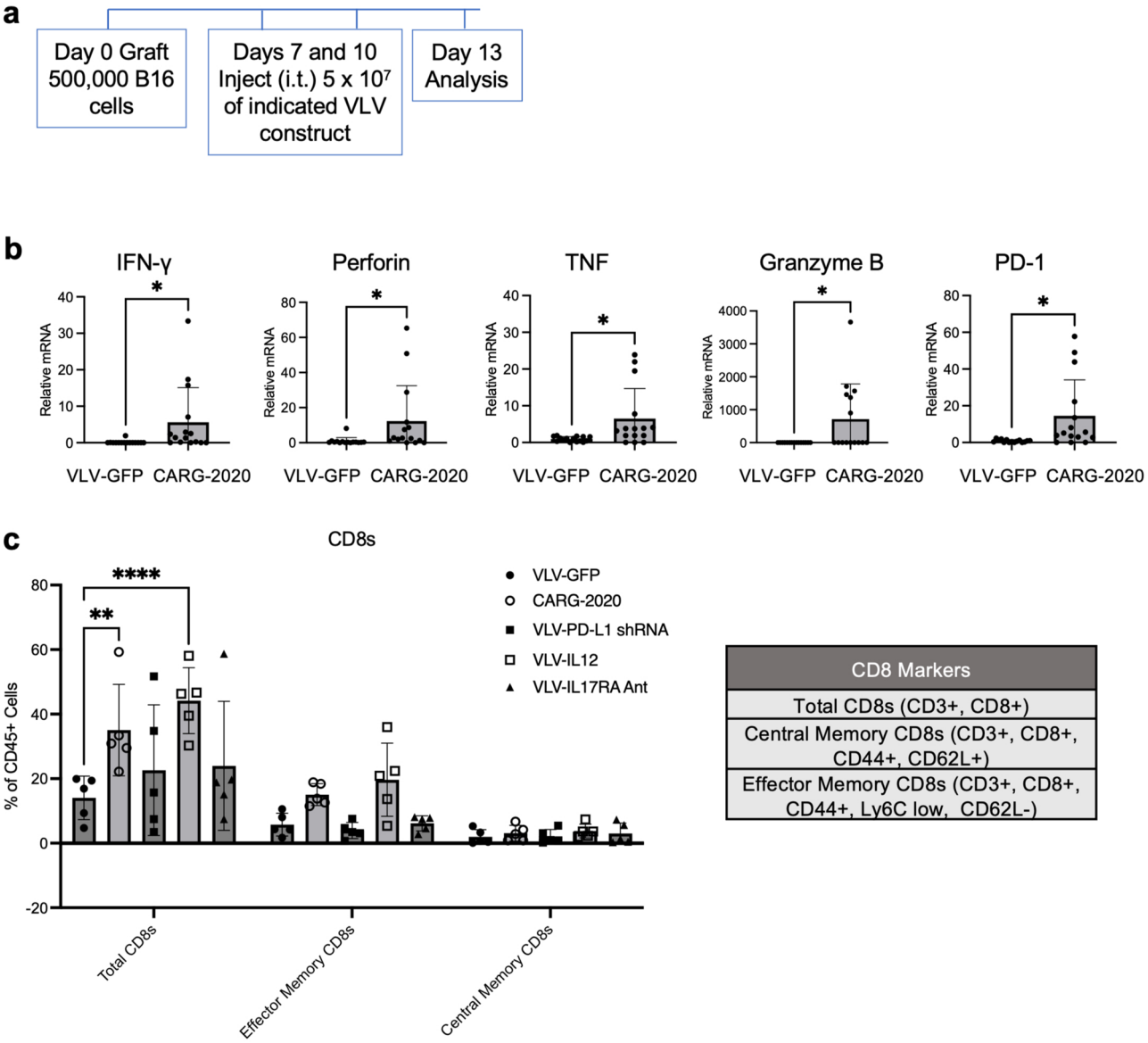

Fig. 7. CARG-2020 activates CD8⁺ T cells in melanoma. **a** 500,000 B16 melanoma cells were grafted subcutaneously into the flank of C57BL/6J mice. At days 7 and 10 after tumor graft, B16 tumors received two injections of indicated VLV agents. Tumors were harvested on day 13 and analyzed by q-RT-PCR for indicated mRNAs (**b**) or flow cytometry for different CD8⁺ cell populations (**c**). * $p < 0.05$, ** $p < 0.01$, *** $p < 0.001$, **** $p < 0.0001$.

Discussion

Cancer immunotherapy has made major progress in the past decade. Immune checkpoint inhibitors, such as those targeting PD-1 or its ligand PD-L1, have been successfully used to treat hitherto untreatable cancers in humans[42]. However, anti-PD-1 or similar agents work only in a small fraction of patients and their resistance has been extensively studied[42]. These resistance mechanisms include T cell exhaustion, metabolism, microbiota, and lack of target (such as PD-L1) expression[42]. In this study, we further expanded the scope of CARG-2020 to include melanoma and TNBC and showed a broad-spectrum efficacy and safety of CARG-2020 across multiple cancer types (Fig. 9). One key component of CARG-2020 is the single-chain biologically active IL-12, which is known to promote Th1-armed immunity[43]. In our previous study, CARG-2020 activated both CD4⁺ and CD8⁺ T cells in tumors[31]. We have shown that when administered to breast tumors (Fig. 8) and colon tumors[31], CARG-2020 was more effective than PD-1 blockade in mice. Activation of T cell-mediated immunity is a plausible cause of such differences, and immunologically cold tumors have been shown to be resistant to immune checkpoint inhibition[44]. The incorporation of an IL-17RA antagonist and PD-L1 shRNAs in CARG-2020 likely further enhances T cell activity and therapeutic efficacy, as shown in our previous study[31]. However, it remains to be seen whether the combined use of CARG-2020 with other immune checkpoint inhibitors will further augment the

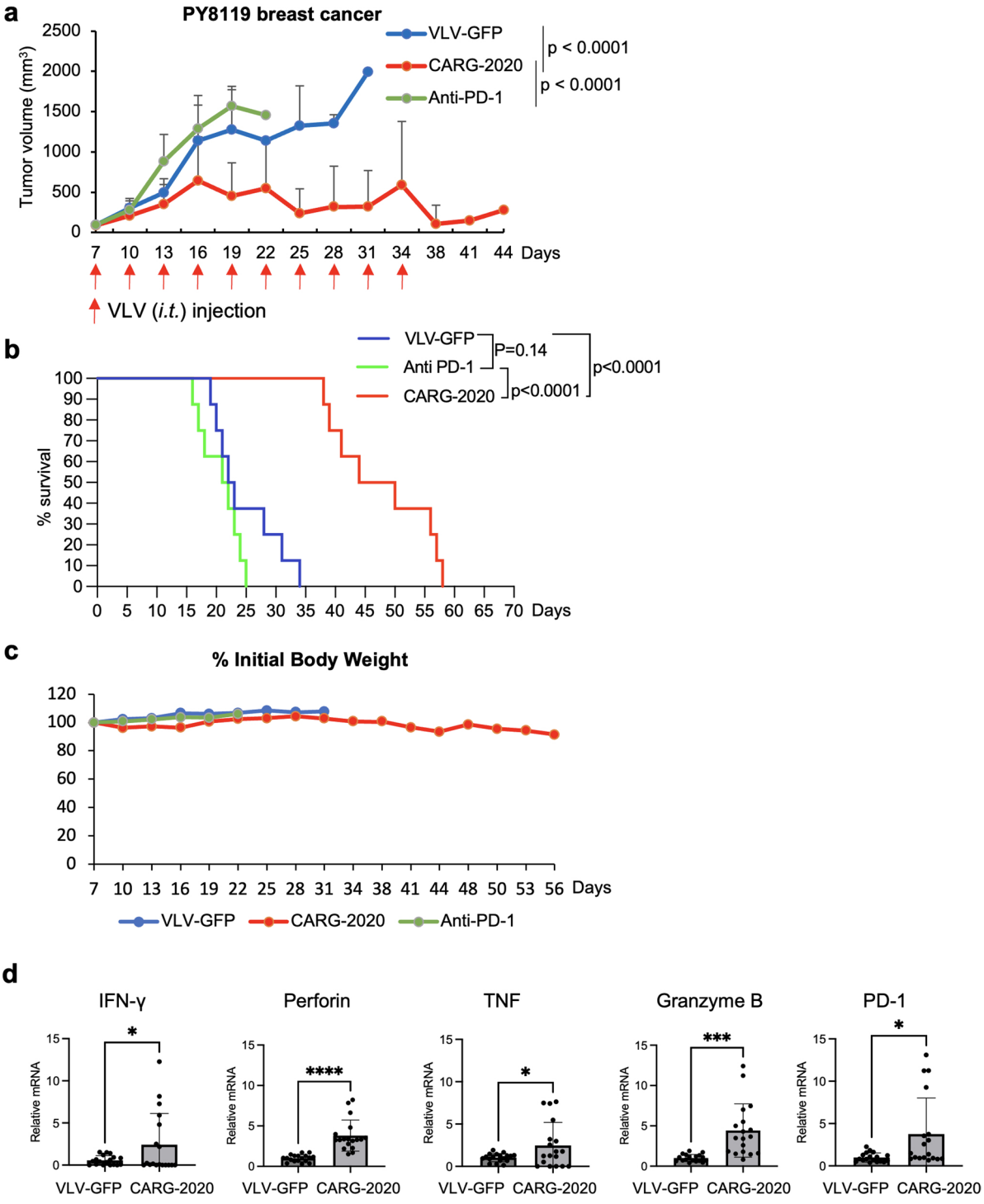

Fig. 8. CARG-2020 is effective against TNBC. 500,000 PY8119 breast cancer cells were grafted to fat pads of the second mammary glands in C57BL/6J mice. 5×10^7 pfu CARG-2020 were injected intratumorally at arrow-indicated time points, along with 100 μg anti-PD-1 antibody which was injected intraperitoneally. **a** Average tumor sizes of mice undergoing indicated treatment. error bar = S.D., $n = 8$. **b** Survival rates of animals undergoing indicated treatment. **c** Average percentages of initial body weight of mice from three treatment groups. $n = 8$. **d** 500,000 PY8119 cells were grafted subcutaneously into the flank of C57BL/6J mice. At days 7 and 10 after tumor graft, tumors received two injections of VLV-GFP or CARG-2020. Tumors were harvested on day 13 and analyzed by q-RT-PCR for indicated mRNAs. * $p < 0.05$, *** $p < 0.001$, **** $p < 0.0001$.

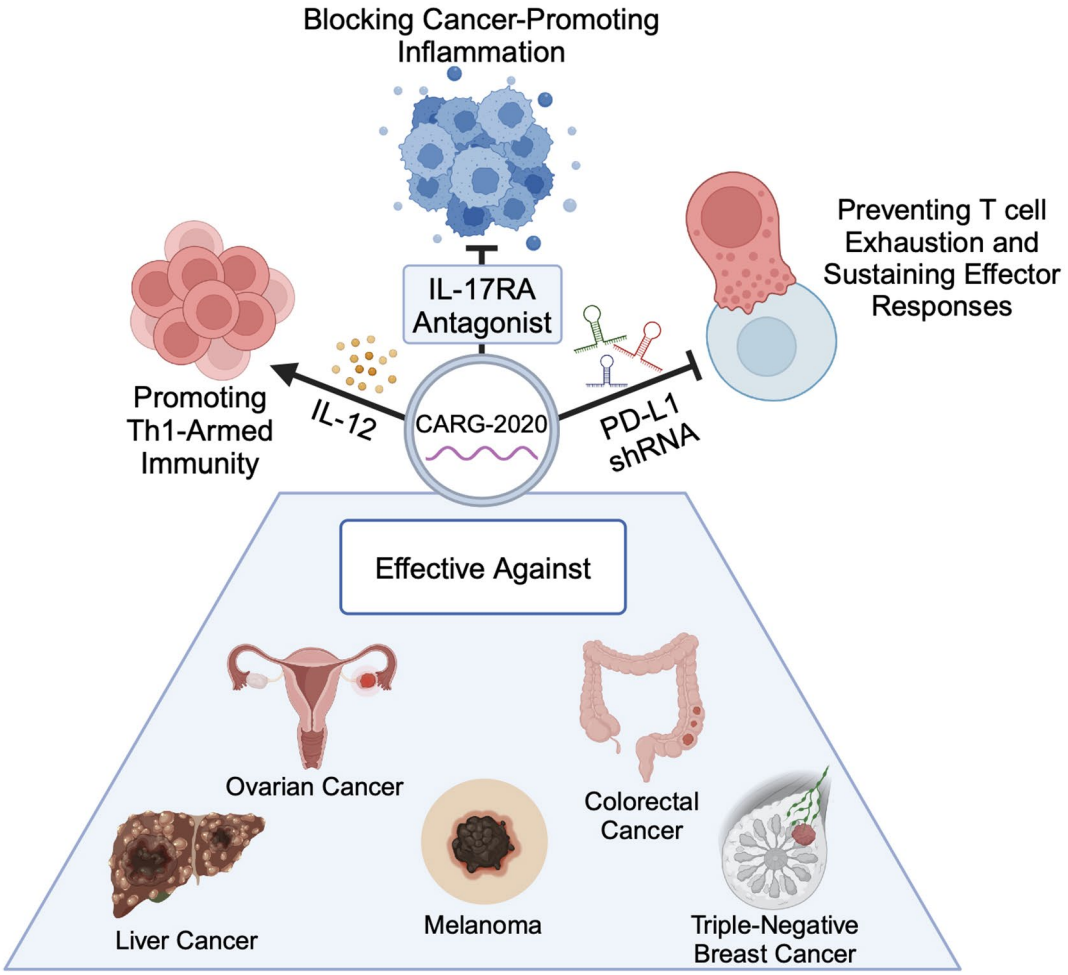

Fig. 9. Broad-spectrum efficacy of CARG-2020 in cancers. CARG-2020 incorporates a single chain, biologically active IL-12 to activate Th1-armed immunity, an antagonist of IL-17RA to block IL-17 signaling and downregulate cancer promoting inflammation, and shRNAs against the immune checkpoint ligand PD-L1. Together, these immune modulating payloads orchestrate to promote robust and long-lasting anti-tumor immune responses. Combined with our previous findings, we now show that CARG-2020 is effective against multiple cancer types, including ovarian cancer, colorectal cancer, liver cancer, melanoma, and triple-negative breast cancer.

cancer-killing potential of the treatment. One promising candidate is the LAG3 inhibitor, whose combination with PD-1 blockade has been shown to be promising in preclinical models and human clinical trials[45,46].

Currently approved oncolytic viral therapies are delivered intratumorally (for T-VEC)[2] and intravesically (for Adstiladrin)[3]. The delivery of viruses via *i.v.* is under development, but may be limited by the tropism and selectivity of the virus, as well as the therapeutic payload(s) that are incorporated therein. With CARG-2020, our study showed that *i.v.* injection of the agent was tolerated at initial doses and effective against established MC38 tumors in mice. However, upon repeated injections, CARG-2020 resulted in treatment-caused deaths in experimental animals. These obervations indicate that in the future clinical development, treatment with CARG-2020 via systemic route should be designed with a conservative dosing scheme with single or few injections to be planned. To emphsize this point, the distribution of VLVs to the spleen upon *i.v.* injection suggests that the therapeutic efficacy of CARG-2020 stems from the delivery of its payload to the peripheral tissues instead of selective targeting to the tumor. It is therefore plausible that i.v. injected CARG-2020 works in an indirect manner to control tumor growth compared to its intratumoral injection.

Based on the data, it is feasible to focus on *i.t.* injection of CARG-2020 at this stage to avoid potential severe adverse events, as observed in the case of IL-12 systemic injection[15–20]. Indeed, systemic delivery of IL-12 has been shown to be toxic in human patients, resulting in a failed Phase II clinical trial and two deaths. Systemic blockade of PD-L1 pathway has been extensively explored in cancer therapies, and blocking IL-17 has been widely used for the treatment of autoimmune disorders such as psoriasis without overt adverse effects[30,47].

Therefore, the toxicity associated with i.v. injected CARG-2020 likely comes from the IL-12 payload, which is confirmed by the exacerbated toxicity associated with i.v. injected VLV-IL-12 (Fig. 3).

One promising way to further enhance the delivery of CARG-2020 is by modifying the VSV-G protein, which guides viral entry into cells. For instance, a recent study showed effective targeting of VSV to $Her2^+$ tumors by removing the LDL-R binding domain on VSV-G and replacing it with a single-chain antibody against Her2[48]. These and other strategies may be employed to selectively target CARG-2020 to tumors and permit systemic injection of the agent, thus further expanding the potential of oncolytic viral therapies for cancer.

Data availability

The data generated in this study are available upon request from the corresponding author.

Received: 25 May 2024; Accepted: 4 August 2025
Published online: 13 August 2025

References

1. Macedo, N. et al. *Clinical landscape of oncolytic virus research in 2020*. *J. Immunother Cancer*, **8**(2). (2020).
2. Andtbacka, R. H. et al. Talimogene Laherparepvec improves durable response rate in patients with advanced melanoma. *J. Clin. Oncol.* **33** (25), 2780–2788 (2015).
3. Boorjian, S. A. et al. Intravesical nadofaragene Firadenovec gene therapy for BCG-unresponsive non-muscle-invasive bladder cancer: A single-arm, open-label, repeat-dose clinical trial. *Lancet Oncol.* **22** (1), 107–117 (2021).
4. Yun, C. O., Hong, J. & Yoon, A. R. Current clinical landscape of oncolytic viruses as novel cancer immunotherapeutic and recent preclinical advancements. *Front. Immunol.* **13**, 953410 (2022).
5. Rolls, M. M. et al. Novel infectious particles generated by expression of the vesicular stomatitis virus glycoprotein from a self-replicating RNA. *Cell* **79** (3), 497–506 (1994).
6. Rose, N. F. et al. Hybrid alphavirus-rhabdovirus propagating replicon particles are versatile and potent vaccine vectors. *Proc. Natl. Acad. Sci. U S A*. **105** (15), 5839–5843 (2008).
7. Rose, N. F. et al. In vitro evolution of high-titer, virus-like vesicles containing a single structural protein. *Proc. Natl. Acad. Sci. U. S. A*. **111** (47), 16866–16871 (2014).
8. Chiale, C. et al. *Modified Alphavirus-Vesiculovirus Hybrid Vaccine Vectors for Homologous Prime-Boost Immunotherapy of Chronic Hepatitis B*. Vaccines (Basel) **8**(2). (2020).
9. Rolls, M. M., Haglund, K. & Rose, J. K. Expression of additional genes in a vector derived from a minimal RNA virus. *Virology* **218** (2), 406–411 (1996).
10. Reynolds, T. D. et al. Virus-Like Vesicle-Based therapeutic vaccine vectors for chronic hepatitis B virus infection. *J. Virol.* **89** (20), 10407–10415 (2015).
11. Yarovinsky, T. O. et al. Virus-like vesicles expressing multiple antigens for immunotherapy of chronic hepatitis B. *iScience* **21**, 391–402 (2019).
12. Hsieh, C. S. et al. Development of TH1 CD4+T cells through IL-12 produced by Listeria-induced macrophages. *Science* **260** (5107), 547–549 (1993).
13. Manetti, R. et al. Interleukin 12 induces stable priming for interferon gamma (IFN-gamma) production during differentiation of human T helper (Th) cells and transient IFN-gamma production in established Th2 cell clones. *J. Exp. Med.* **179** (4), 1273–1283 (1994).
14. Knutson, K. L. & Disis, M. L. Tumor antigen-specific T helper cells in cancer immunity and immunotherapy. *Cancer Immunol. Immunother*. **54** (8), 721–728 (2005).
15. Colombo, M. P. & Trinchieri, G. Interleukin-12 in anti-tumor immunity and immunotherapy. *Cytokine Growth Factor. Rev.* **13** (2), 155–168 (2002).
16. Vizler, C. et al. Therapeutic effect of Interleukin 12 on mouse haemangiosarcomas is not associated with an increased anti-tumour cytotoxic T-lymphocyte activity. *Br. J. Cancer*. **77** (4), 656–662 (1998).
17. Noguchi, Y. et al. Effect of Interleukin 12 on tumor induction by 3-methylcholanthrene. *Proc. Natl. Acad. Sci. U. S. A*. **93** (21), 11798–11801 (1996).
18. Zaharoff, D. A. et al. Intratumoral immunotherapy of established solid tumors with chitosan/IL-12. *J. Immunother*. **33** (7), 697–705 (2010).
19. Younes, A. et al. Phase II clinical trial of interleukin-12 in patients with relapsed and refractory non-Hodgkin's lymphoma and hodgkin's disease. *Clin. Cancer Res.* **10** (16), 5432–5438 (2004).
20. Nguyen, K. G. et al. Localized Interleukin-12 for cancer immunotherapy. *Front. Immunol.* **11**, 575597 (2020).
21. McGeachy, M. J., Cua, D. J. & Gaffen, S. L. The IL-17 family of cytokines in health and disease. *Immunity* **50** (4), 892–906 (2019).
22. Meehan, E. V. & Wang, K. *Interleukin-17 family cytokines in metabolic disorders and cancer*. *Genes (Basel)*, **13**(9). (2022).
23. Wang, K. et al. Interleukin-17 receptor a signaling in transformed enterocytes promotes early colorectal tumorigenesis. *Immunity* **41** (6), 1052–1063 (2014).
24. Chae, W. J. et al. Ablation of IL-17A abrogates progression of spontaneous intestinal tumorigenesis. *Proc. Natl. Acad. Sci. U. S. A*. **107** (12), 5540–5544 (2010).
25. Grivennikov, S. I. et al. Adenoma-linked barrier defects and microbial products drive IL-23/IL-17-mediated tumour growth. *Nature* **491** (7423), 254–258 (2012).
26. Song, X. et al. Alterations in the microbiota drive interleukin-17 C production from intestinal epithelial cells to promote tumorigenesis. *Immunity* **40** (1), 140–152 (2014).
27. Chae, W. J. & Bothwell, A. L. IL-17F deficiency inhibits small intestinal tumorigenesis in apcmin/++ mice. *Biochem. Biophys. Res. Commun.* **414** (1), 31–36 (2011).
28. Coffelt, S. B. et al. IL-17-producing gammadelta T cells and neutrophils conspire to promote breast cancer metastasis. *Nature* **522** (7556), 345–348 (2015).
29. Chen, J. et al. IL-17 inhibits CXCL9/10-mediated recruitment of CD8(+) cytotoxic T cells and regulatory T cells to colorectal tumors. *J. Immunother Cancer*. **7** (1), 324 (2019).
30. Zou, W., Wolchok, J. D. & Chen, L. PD-L1 (B7-H1) and PD-1 pathway blockade for cancer therapy: Mechanisms, response biomarkers, and combinations. *Sci. Transl. Med.* **8**(328), 328rv4 (2016).
31. Chen, J. et al. Cancer immunotherapy with enveloped self-amplifying mRNA CARG-2020 that modulates IL-12, IL-17 and PD-L1 pathways to prevent tumor recurrence. *Acta Pharm. Sin B*. **14** (1), 335–349 (2024).
32. Lin, X. et al. Regulatory mechanisms of PD-1/PD-L1 in cancers. *Mol. Cancer*. **23** (1), 108 (2024).
33. Han, Y., Liu, D. & Li, L. PD-1/PD-L1 pathway: Current researches in cancer. *Am. J. Cancer Res.* **10** (3), 727–742 (2020).
34. Alvero, A. B. et al. Immune modulation of innate and adaptive responses restores immune surveillance and establishes antitumor Immunologic memory. *Cancer Immunol. Res.* **12** (2), 261–274 (2024).

35. Senkus, E. et al. Primary breast cancer: ESMO clinical practice guidelines for diagnosis, treatment and follow-up. *Ann. Oncol.* **26** (Suppl 5), v8–30 (2015).
36. Fayaz, S. et al. Triple negative breast cancer: 10-Year survival update of the applied treatment strategy in Kuwait. *Gulf J. Oncol.* **1** (29), 53–59 (2019).
37. Sharma, P. Biology and management of patients with Triple-Negative breast cancer. *Oncologist* **21** (9), 1050–1062 (2016).
38. Abdou, Y. et al. Immunotherapy in triple negative breast cancer: Beyond checkpoint inhibitors. *NPJ Breast Cancer*. **8** (1), 121 (2022).
39. Liu, Y. et al. Advances in immunotherapy for triple-negative breast cancer. *Mol. Cancer*. **22** (1), 145 (2023).
40. Bonaventura, P. et al. Cold tumors: A therapeutic challenge for immunotherapy. *Front. Immunol.* **10**, 168 (2019).
41. Maleki Vareki, S. High and low mutational burden tumors versus immunologically hot and cold tumors and response to immune checkpoint inhibitors. *J. Immunother Cancer*. **6** (1), 157 (2018).
42. Vesely, M. D., Zhang, T. & Chen, L. Resistance mechanisms to Anti-PD cancer immunotherapy. *Annu. Rev. Immunol.* **40**, 45–74 (2022).
43. Lieschke, G. J. et al. Bioactive murine and human interleukin-12 fusion proteins which retain antitumor activity in vivo. *Nat. Biotechnol.* **15** (1), 35–40 (1997).
44. Zhang, J. et al. Turning cold tumors hot: From molecular mechanisms to clinical applications. *Trends Immunol.* **43** (7), 523–545 (2022).
45. Woo, S. R. et al. Immune inhibitory molecules LAG-3 and PD-1 synergistically regulate T-cell function to promote tumoral immune escape. *Cancer Res.* **72** (4), 917–927 (2012).
46. Schoffski, P. et al. Phase I/II study of the LAG-3 inhibitor Ieramilimab (LAG525) +/- anti-PD-1 Spartalizumab (PDR001) in patients with advanced malignancies. *J. Immunother Cancer*, **10**(2). (2022).
47. Huangfu, L. et al. The IL-17 family in diseases: From bench to bedside. *Signal. Transduct. Target. Ther.* **8** (1), 402 (2023).
48. Gao, Y. & Bergman, I. Vesicular stomatitis virus (VSV) G glycoprotein can be modified to create a Her2/Neu-Targeted VSV that eliminates large implanted mammary tumors. *J. Virol.* **97** (6), e0037223 (2023).

Acknowledgements

We thank Dr. Weizhou Zhang from the University of Florida for providing us the PY8119 cell line and expertise in breast cancer mouse models. We also thank Dr. Evan Jellison and Zhu Li from the Flow Cytometry Core Facility of UConn Health for technical support. This work was supported by the American Association of Immunologists Careers in Immunology Fellowship to Ju Chen, the University of Connecticut Innovation Fund to Valerian Nakaar and Kepeng Wang, and the National Institute of Health/National Cancer Institute (NIH/NCI R01CA262430, USA) to Kepeng Wang. This research was also funded by NIH/NIDDK (R44DK113858, USA), and NIAID (No. R43AI149798, USA) to Valerian Nakaar. The content is the sole responsibility of the authors and does not necessarily represent the official views of the National Institutes of Health. The funders had no role in the study design, data collection, interpretation, or decision to submit the manuscript for publication.

Author contributions

B.A., V.N., and K.W. conceived the project. E.A., C.C, B.R.M., M.M.K., and J.C. performed experiments and analyzed the data. T.O.Y. provided conceptual advice and analyzed the data. E.A., C.C., B.R.M., V.N., and K.W. wrote the manuscript. All authors contributed to writing, editing, and providing key advice.

Declarations

Competing interests

Kepeng Wang is a member of the Scientific Advisory Board of the CaroGen Corporation. Elham Ahmadi, Bhaskara Reddy Madina, Timur Olegovich Yarovinsky, Marie Marthe Krady, Valerian Nakaar, and Bijan Almassian are current or former employees of CaroGen Corporation. The authors declare no additional financial interests.

Additional information

Correspondence and requests for materials should be addressed to K.W.